Article

Application of Empirical Approaches for Fast Landslide Hazard Management: The Case Study of Theilly (Italy)

Samuele Segoni * , Francesco Barbadori , Alessio Gatto and Nicola Casagli

Department of Earth Sciences, University of Florence, 50121 Florence, Italy
* Correspondence: samuele.segoni@unifi.it

Abstract: Landslide hazard management usually requires time-consuming campaigns of data acquisition, elaboration, and modeling. However, in the post-emergency phase management, time is a factor, and simpler but faster methods of analysis are needed to support decisions even in the short-term. This paper analyzes the Theilly landslide (Western Italian Alps), which was recently affected by a series of reactivations. While some instrumental campaigns are being carried out to support the design of protection measures, simple tools are also needed to assess the hazard of future reactivations and to evaluate the possibility of damming the torrent at the footslope. Therefore, state-of-the-art empirical methods were used and customized for the specific case study: a set of intensity–duration rainfall thresholds depicting increasing hazard levels was defined to monitor and forecast possible reactivations, while a methodology based on hydro-morphometric indices was applied to the case of study, to assess the possible evolution scenarios (landslide that does not dam the river, formation of a stable dam, formation of an unstable dam), based on the landslide volume. The proposed empirical methodologies have the advantage of requiring only ready-available input data and quick elaborations, thus allowing the rapid set up of tools that could be used for hazard management.

Keywords: landslide; hazard; risk; Alps; rainfall threshold; landslide dam; empirical methods; morphometric index

1. Introduction

Landslides are a serious threat to life, buildings and infrastructures [1–3]; in addition, in specific environments they may be responsible for disastrous cascading events such as river damming (and subsequent outbursts) [4–7]. Landslide characteristics vary deeply according to the nature of the geomorphological setting and the external triggering and predisposing factors. Therefore, the correct management of landslide risk in a given case of study requires the acquisition of information and the performance of a site-specific analysis by means of instrumental investigations, monitoring, sophisticated physical models, and powerful software programs. However, it is usually time consuming to get reliable input data, design and carry out investigations, process the data, and perform analyses. For this reason, empirical methods are viable options to get preliminary results and, although consisting mostly in simplified approaches, they have been established in many fields of landslide research. For instance, empirical rainfall thresholds are widely used instead of physically based models to assess the timing of occurrence of landslides and to set up early warning systems [8,9]. Physically based models are undoubtedly more rigorous and sophisticated, but their use is limited by the difficulty of getting reliable input data with sufficient accuracy for the many input parameters they require [8,10,11]. For this reason, the simpler approach based on empirical rainfall thresholds is the most widely employed in operational civil protection procedures for landslide hazard forecasting and management [12,13]. Caine [14] was the first to establish an empirical relationship between two simple rainfall parameters (namely, intensity and duration) and shallow landslide

occurrence across the world. Since then, the empirical rainfall threshold approach gained popularity and was used also for operational implementations into warning systems [15] and several successful applications are reported [16–18].

Another example is the analysis of river damming by landslides occurring in narrow valleys: the possibility of formation of a dam and its evolution (i.e., the permanent creation of a lake or its collapse with release of flood waves) is a very complex task that requires the definition of a geological conceptual model of the landslide and the use of complex models, which in turn requires the definition of many geotechnical and hydrological input parameters [19–21]. For this reason, several authors proposed empirical indices that can be used to assess the damming potential of landslides [22–25]: such indices are usually based on a combination of morphometric, geotechnical and hydrological attributes and can be used for a fast estimation of river damming hazard [26]. For instance, [22] proposed two indices based on the ratio between the landslide volume and the drained surface and on the ratio between the valley width and the landslide velocity to account for the river blockage and the subsequent material removal by the flowing water. In the years, other indices were proposed, and an interesting direction of applied research was to identify parameters empirically linked with landslide dam evolution but, at the same time, being straightforward enough to assess to maximize the potential applicability of the technique. For instance, [23] proposed a dimensionless blockage index based on the dam height, the landslide volume, and the upslope catchment area, arguing that all these parameters could be easily estimated by means of a field survey or GIS analyses, thus allowing for a quick hazard assessment.

The main objective of this manuscript is to showcase the practical utility of expeditious empirical methods by describing and discussing the case of the Theilly landslide, located in the Western Italian Alps. The Theilly landslide has a complex history of reactivations, and while investigation and complex analysis are promoted to gain a deeper understanding of the slope setting, to design and execute a more effective generation of remedial works, there is the need to immediately address the risks associated with possible reactivations and cascading effects including river damming. Thus, given also the absence of previous research published on the site, the objective of this work is to establish a simple method to monitor and forecast the possible evolution of the landslide with easily available data and make use of consolidated but simple empirical methodologies, while in the meantime more thorough investigations are carried out to assist more complex methods of analysis and the design and implementation of effective countermeasures.

Test Site Description

The study area is located in northern Italy (Figure 1a) in the municipality of Fontainemore (AO), on the right bank of the Lys stream, immediately upstream from the confluence with the Theilly stream (Figure 1b). The morphology of the valley was formerly shaped by glacial activity until the Pleistocene, afterwards it was deeply engraved by the Lys stream, assuming a typical V-shape in the lower part of the mountainsides.

The slope affected by the landslide is very steep, except for a nearly flat glacial terrace near the village of Theilly (about 840–850 m asl) just above the landslide crown (Figure 1c). The slope has a thick cover of sediments of mixed origin, including sedimentary bodies of glacial origin (with a medium-fine matrix), slope debris coming from the upslope sectors (coarse debris with blocks and boulders), weathered regolith derived from the gneissic bedrock, and anthropogenic fill soil.

Erosive processes are active on the slope. They are partly mitigated by the effect of the vegetation, where present, and are particularly intense at the edge of the terrace. In the nearby sectors of the slope, the evidence of past landslides activity is also present.
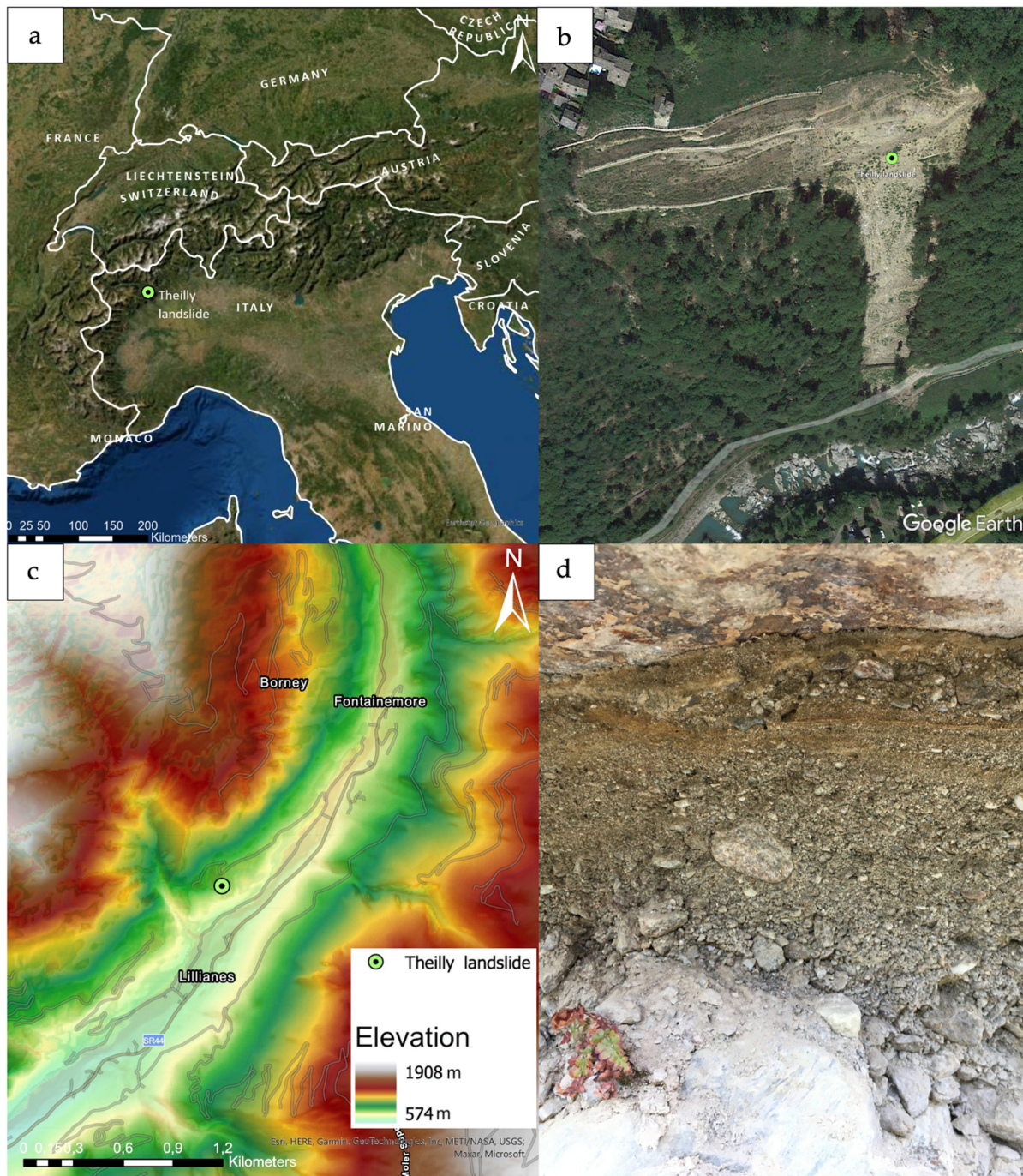
Figure 1. (**a**) Location of Theilly landslide, Western Alps, northern Italy; (**b**) Theilly landslide, the green point identifies the head of the scarp; (**c**) DTM of the valley where Theilly landslide is located (**d**) Detail of the heterogenic sedimentary cover of the slope.

To protect the village from erosion and landslide processes, in 2011 some remedial works began, but they were not completed as in 2016 a major landslide was triggered by a very intense rainstorm (25–28 September 2016) (Figure 1b). The landslide was a shallow planar debris slide that partially dislocated the filling material and the remedial works (mainly gabions) under construction. The slope stayed in a quiescent state of activity until 2019, with some minor slides occurring in autumn 2018 and spring 2019 after intense rainfall events. On 24 November 2019, due to exceptionally intense rainfalls, a major planar slide was triggered again in the debris cover of the slope, and the saturated material evolved in a slow debris flow, partially reaching the Lys stream.

At present, local authorities are promoting geotechnical and geophysical investigations to gain a deeper understanding of the slope structure, to assist the design and the implementation of more effective remedial works. However, in the meantime, there is the urgency to quickly develop simple tools to manage the landslide hazard related to possible reactivation of landslides and the possibility of damming the Lys stream at the footslope. These concerns justified the adoption of the simple but "ready-to-use" empirical methodologies described in the following sections, to be temporarily used until the main analysis and remedial works are completed.

2. Materials and Methods

2.1. Rainfall Threshold Analysis

Rainfall thresholds are mathematical equations, usually defined by empirical methods, defining the rainfall conditions associated with the occurrence of landslides [9]. The rainfall threshold model used for this study is the widely acknowledged intensity–duration (*I–D*) power law relationship, firstly proposed by Caine [14], and still at present the most used worldwide [9]:

$$I = \alpha * D^{-\beta} \tag{1}$$

where *I* [mm/h] is the intensity of the triggering rainfall event, *D* [hours] is the duration of the triggering rainfall event, α and β are dimensionless empirical parameters, specific of the study area. The equation can be represented in a bi-logarithmic diagram with a straight line that divides the stability condition field (under the threshold) and the rainfall conditions associated with previous landslide occurrences (above the threshold). Among the many possible rainfall parameters used in the literature [9], *I* and *D* were chosen also because they are considered the most appropriate in the case of shallow landslides on relatively permeable material, which have a rapid and straightforward response to intense peaks of precipitation [27,28]. It was verified by a field survey that the Theilly slope matches these characteristics. Moreover, the analysis of pluviographs and reports of past events highlighted that, in all the documented reactivations, the role of antecedent rainfall was negligible, snow melting processes were absent, and the main triggering factor was a relatively short but very intense rainfall.

After selecting the rainfall threshold model, it was necessary to gather the input data for the threshold definition. The input data consist of a dataset of past landslide occurrences with known time and location and a dataset of rainfall measures to extract the rainfall conditions that led to slope instabilities.

There is not a consensus on what is the minimum number of events to calibrate a threshold: the literature accounts for rainfall thresholds calibrated with hundreds or thousands of landslide events [29–34], as well as thresholds calibrated with less than 10 events [35,36]. In any case, we considered that the only known reactivations of Theilly landslides (three major events and four minor ones) were not enough for a robust calibration, also because a robust threshold analysis demands that a certain number of events is excluded from the calibration process to perform an independent validation. Consequently, the calibration dataset was built considering the largest possible number of landslide events occurred in the vicinity of Theilly, in similar geological and meteorological settings, while Theilly reactivations were used to validate the threshold and to assess its forecasting effectiveness.

The landslide event dataset was built using a web datamining algorithm based on a semantic search engine applied to internet news [37]. This method detects landslide news on the Internet and has the intrinsic feature of identifying only events that resulted in significant impacts, which had a resonance on the media, making it a good source of information for model validation [38]. This method allowed compiling a dataset of 20 internet new items related to 12 landslides that occurred in the period 2010–2019 and that are located in an area that can be considered near and similar to the test site (Figure 2). The landslides news days used for the extraction and calibration of the threshold are presented in Table 1.
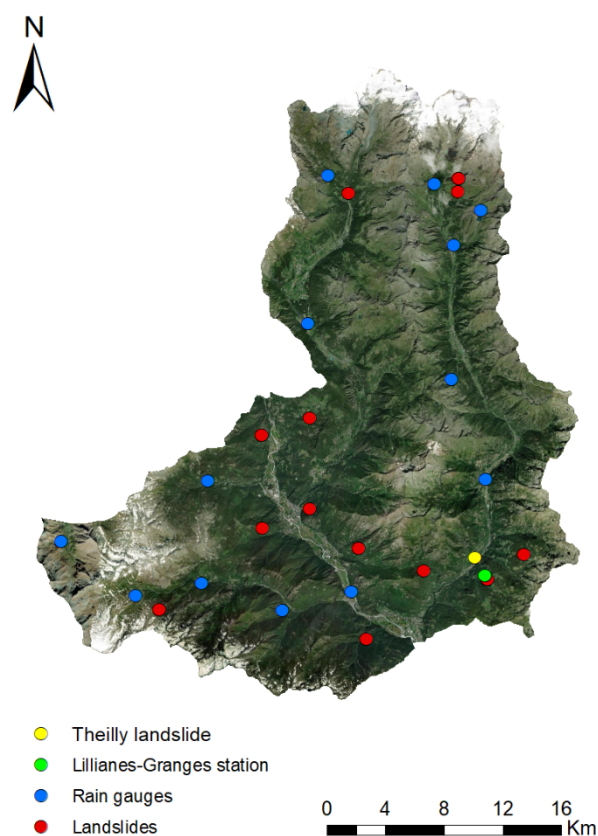
Figure 2. Overview of the rainfall and landslide data collected in the same physiographic setting of Theilly landslide.

Table 1. Landslides news used for the calibration.

Day of Landslide Occurrence
3 September 2012
3 September 2012
17 May 2013
25 June 2016
23 November 2016
25 March 2017
4 September 2017
12 January 2018
29 May 2018
11 June 2018
1 November 2018
22 November 2019

The selection of the measuring rain gauge is a critical point in the rainfall analysis [9,39–41]. The hourly rainfall measurements from the regional rain gauge network were used to characterize the triggering rainfall of the landslide calibration dataset. In particular, the Lillianes–Granges's rain gauge was chosen as a reference to characterize the rainfalls that reactivated the Theilly landslide and to validate the applicability of the threshold to the specific case of Theilly. This rain gauge was selected as it is the nearest to Theilly landslide (1.3 km distance), at similar elevation and in the same valley, just in front of the unstable slope (Figure 2).

The input data were processed with a tool called MaCumBA (Massive Cumulative Brisk Analyzer) [42], which automatically matches rainfall and landslide data, analyzes the triggering rainfall records, selects for each landslide the most appropriate rain gauge and extracts the intensity and the duration of the triggering rainfall. The *I–D* couples for every

landslide are plotted in a bi-logarithmic graph and a statistical threshold is identified with a specific confidence level (95% in this work). Further details on the method can be found in [42].

2.2. Landslide Dam Analysis

To provide useful elements for the understanding and management of multi-risk scenarios concerning the interaction between the landslide and the dynamics of the watercourse flowing at the foot of the slope, the case study was characterized by a series of state-of-the-art hydro-morphometric indices. These indices are commonly used as fast methods in preliminary investigations to estimate, in the event of a landslide that reaches a watercourse, which one of the following scenarios is more likely: no river dam formation, the formation of a stable river dam, or the formation of an unstable river dam. A methodology recently developed by [26] was selected for the analyses, because of the advantage of being based on the joint use of two morphometric indices that are easy to assess, as the data needed can be quickly collected from field surveys and GIS analysis on widely available data [26].

The first index, called *MOI* (Morphological Obstruction Index), is defined as follows:

$$MOI = log\left(\frac{V_l}{W_v}\right) \tag{2}$$

where V_l [m^3] is the volume of the landslide and W_v is the width of the valley [m]. The index can be used to estimate the volume that is capable of generating a river dam according to [26]:

- *MOI* < 3.00 non-formation domain
- 3.00 < *MOI* < 4.60 uncertainty domain
- *MOI* > 4.60 formation domain

The second index, the Hydromorphological Dam Stability Index (*HDSI*), is defined as follows:

$$HDSI = log\left(\frac{V_l}{tan\ (S)\ *\ A_b}\right) \tag{3}$$

where V_l [m^3] is the volume of the landslide, S [°] is the local slope of the waterbed and A_b [km^2] is the upslope contributing area subtended by the point affected by the possible dam. The product between S and A_b is commonly used in hydrology and geomorphology to characterize the erosive power of water courses. The relationship with the volume of the landslide allows to estimate the conditions that lead the erosive power of the river to prevail over the landslide body and, consequently, to characterize the stability or instability of any river dam generated by a landslide. The threshold values identified by [26] are as follows:

- *HDSI* > 7.44 stability domain
- 7.44 < *HDSI* < 5.74 uncertainty domain
- *HDSI* < 5.74 instability domain

The threshold values of the *MOI* and *HDSI* were defined by [26] following an analysis based on a dataset of hundreds of cases of river dams documented in Italy. These analyses made it possible to develop and test, with statistical techniques, a methodology for the combined use of the *MOI* and *HDSI* indices, allowing to determine a series of critical volumes that can be interpreted as threshold values to discriminate between the three possible states of evolution that could occur if the landslide reaches the watercourse at the foot of the slope: no river dam formation, the formation of a stable dam, or the formation of an unstable dam [26].

The geomorphological parameters in Equations (2) and (3) (namely, W_v, S, and A_b) were extracted from open-access high resolution DTMs (Digital Terrain Models) provided by the Valle d'Aosta Region. After a field survey and an analysis of the ancillary data

(DTMs and a 1:5000 topographic map), the critical hydraulic section for a possible river dam at the foot of the unstable slope was identified as in Figure 3, in correspondence with an artifact that protects the banks from erosion but also diminishes the hydraulic section. ArcGIS Pro® software was used to assess the hydro-morphometric parameters was used to calculate the hydro-morphometric parameters in correspondence of the critical section, identified as possible damming point (Figure 3). Then, their values were entered in Equations (1) and (2), in which the *MOI* and *HDSI* were also substituted by the threshold values identified by [26]. Finally, Equations (1) and (2) were solved for the volumes, in order to identify the threshold volumes that separate the possible states of evolution of a river dam.
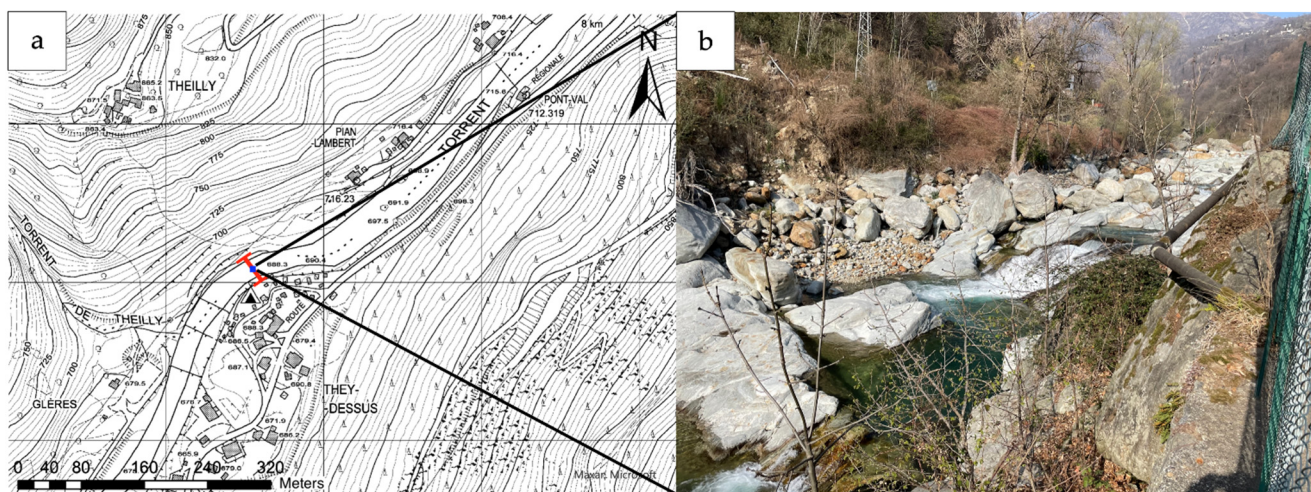
Figure 3. (**a**) Detail of the 1:5000 topographic map representing Theilly area; the critical section is highlighted in red and the point used for DTM analysis is represented in blue; (**b**) Photograph of the critical section, where an anthropic element is present.

3. Results

3.1. Rainfall Threshold Analysis

The first result of the rainfall threshold analysis described in the previous section was a rainfall threshold defined by the following equation:

$$I = 6.71 * D^{-0.67} \tag{4}$$

This threshold is intentionally conservative, because the calibration procedure was carried out setting a relatively low (5%) proportion of rainfall events associated with landslides that fall below the threshold (missed alarms), which usually comes at the cost of many errors of commission (false positives—events above the threshold, but without landslides). Therefore, this threshold may be interpreted as the minimum rainfall conditions associated to the triggering of landslides and cannot be used effectively for warning purposes.

To pass from the triggering threshold defined by MaCumBA to a warning model, the empirical procedure proposed by [29] was taken into account and customized for the case study at hand, taking also into account the effect of non-landslide events and the existing civil protection procedures operated in Italy. The threshold defined by MaCumBA was considered as the base threshold of a set of three thresholds defining four criticality states. The base threshold (Equation (4)) was used to separate the "absent criticality level" state from the "ordinary criticality level". Then, the threshold was translated upward to find two higher thresholds and define increasing warning levels ("moderate criticality" and "high criticality" levels). In this work, the procedure was guided by the necessity of empirically linking the thresholds to different degrees of frequency of possible errors of commission (i.e., false positives, or false alarms). Thus, the thresholds and subsequently the states of the system were defined based on the progressive filtering of the false alarms obtained in the

calibration dataset. In particular, the moderate criticality threshold was defined translating upward the base threshold until only an average of one false alarm per year would be committed (10 events above the threshold without any triggered landslide). For the high criticality threshold, the translation ended when no false alarms were committed in the calibration dataset.

At the end of the procedure, the following equations (Equations (5) and (6)) completed the set of thresholds identified for the study area.

$$I = 29 * D^{-0.67} \text{ (moderate criticality threshold)} \tag{5}$$

$$I = 66 * D^{-0.67} \text{ (high criticality threshold)} \tag{6}$$

The set of the rainfall thresholds, with the corresponding calibration data, are represented in Figure 4 and Table 2.
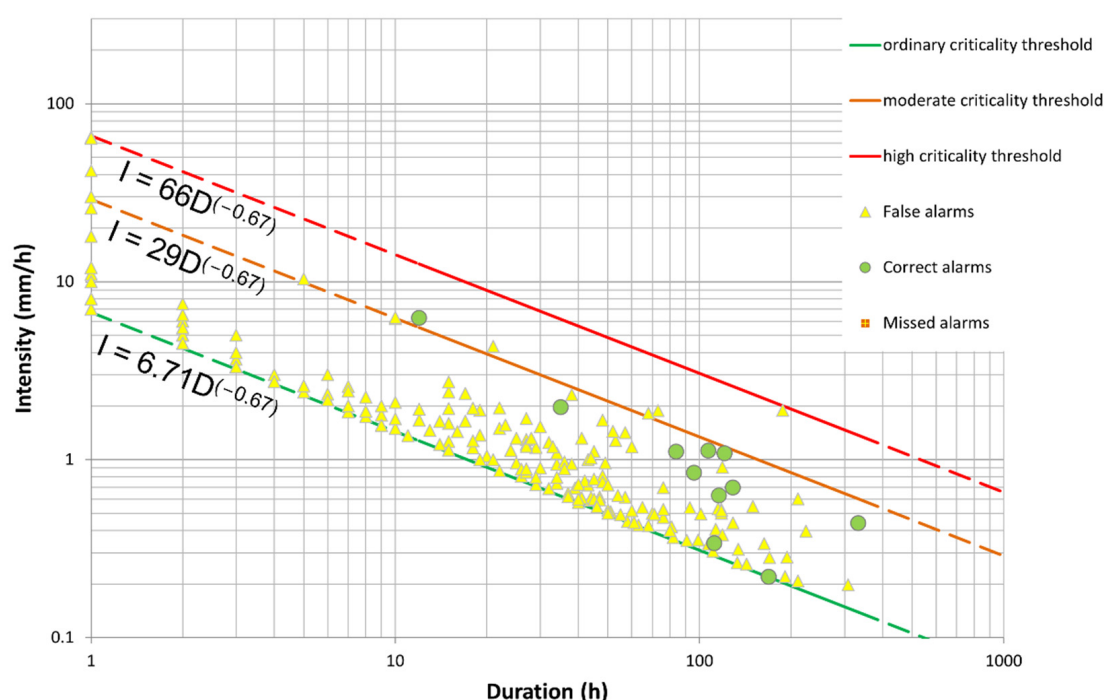

Figure 4. The set of rainfall thresholds and the calibration dataset of events.

Table 2. Rainfall events associated with landslides in the calibration period.

End Day of the Event	Intensity (mm/h)	Duration (h)	Amount of Rain (mm)
5 September 2012	0.22	169	37
5 September 2012	0.22	169	37
19 May 2013	1.12	107	120
25 June 2016	6.25	12	75
25 November 2016	0.84	96	81
26 March 2017	1.11	84	93
5 September 2017	0.34	112	38
13 January 2018	0.44	333	146
31 May 2018	0.63	116	73
12 June 2018	1.97	35	69
1 November 2018	1.08	121	131
27 November 2019	0.70	129	90

The effectiveness of the thresholds set as a possible warning system for the Theilly landslide was evaluated using the reactivation events of the Theilly landslide from 2016 to

present as a validation dataset (Table 3). The reactivation events were split in two groups: "major events" (landslide events with a consistent displacement of material along the slope and/or with damages to the protection structures) and "minor events" (landslide events with lesser amounts of material mobilized and no damages to the existing structures).

Table 3. Theilly landslide reactivation events.

Theilly Landslide Events	
25 November 2016	major and first activation
11 October 2018	minor event
7 November 2018	minor event
4 and 7 April/2019	two minor events
24 November 2019	major event
3 October 2020	major event

The reactivation events were characterized in terms of intensity and duration of the triggered rainfall event, as shown in Tables 4 and 5, and they were compared with the rainfall thresholds (Figure 5).

Table 4. Rainfall events associated with major reactivations.

End Day of the Event	Intensity (mm/h)	Duration (h)	Amount of Rain (mm)
25 November 2016	3.46	102	353
27 November 2019	1.43	130	186
4 October 2020	3.96	70	277

Table 5. Rainfall events associated with minor reactivations.

End Day of the Event	Intensity (mm/h)	Duration (h)	Amount of Rain (mm)
11 October 2018	2.97	34	101
7 November 2018	2.72	247	671
4 April 2019	1.98	41	81
7 April 2019	3.82	11	42

Figure 5 highlights that the proposed set of thresholds is in accordance with the activity of Theilly landslide. Indeed, all the reactivation events are above the ordinary criticality threshold (thus, there are not missed alarms). Furthermore, all the "major events" are plotted at least above the moderate criticality threshold and the most critical events, namely the 2016 event and the 2020 event, are plotted above the high criticality threshold (within the maximum warning level). The other major event (2019 event) is plotted above the moderate criticality threshold inside the moderate warning level. Regarding the "minor events", two of them fall inside the ordinary warning level, one above the moderate criticality threshold and one above the high criticality threshold.

The validation shows satisfactory outcomes also concerning the false alarms that would have been issued in the case of the use of the proposed set of thresholds at Theilly. As expected, a relatively high number of false alarms (namely, 39) are present at the "ordinary criticality" level: as anticipated, this is normal in the case of a minimum threshold for possible activations, not to be used for operational response. Concerning the moderate criticality level, only one false alarm (11 May 2021 event) is committed, in accordance with the criteria used in the calibration. Conversely, the higher state of alert has one false alarm that occurred on the 9 January 2018. In this case, the calibration criterion is not satisfied but the error committed is conservative (i.e., hazard is overestimated), thus allowing for the use of the threshold system as a cautionary operational tool for hazard management.
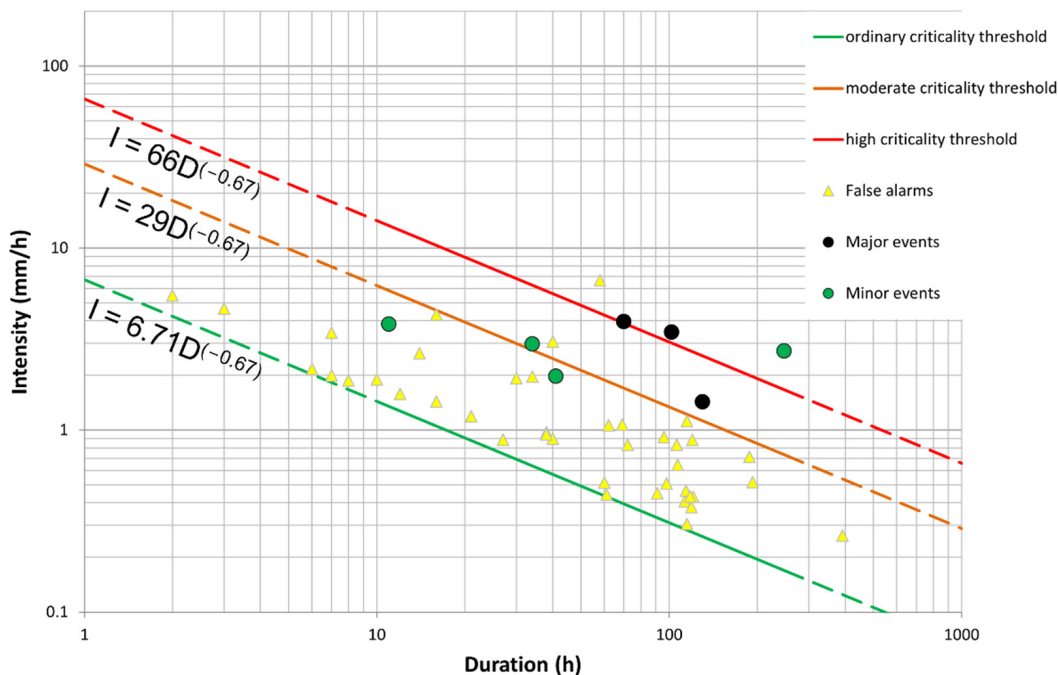
Figure 5. Comparison between the proposed set of rainfall thresholds and the validation dataset, providing evidence of correctly forecasted major events (black dots), correctly forecasted minor events (green dots), and false alarms (yellow triangles).

3.2. Landslide Dam Analysis

3.2.1. *MOI* Index Analysis

The result of this analysis consisted in deriving the critical landslide volumes for the formation and non-formation of a river dam. The two domains can be viewed in Figure 6, which shows a graph with the values of W_v on the abscissas and the values of V_l on the ordinates. According to [26], two lines with equations $V = 180.3\,W^2$ and $V = 1.7\,W^{2.5}$ separate the three domains of dam formation. Using ArcGIS Pro® software, the width of the critical section was measured, obtaining $W_v = 36.15$ m.
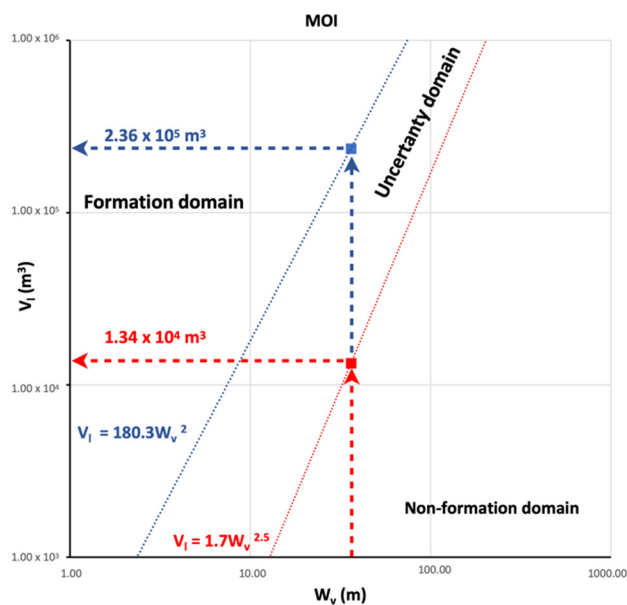
Figure 6. *MOI* parameter graph, the red and blue points correspond to the critical landslide volumes (V_l) for the two domains.

Knowing the value of the valley width, the threshold volumes of the two domains in the case of Theilly landslide were calculated:

Threshold volume of the formation domain (formation of a barrier for higher volumes): $V_{l\,form}$ = approximately 236,000 m^3

Threshold volume of the non-forming domain (no barrier formation for lower volumes): $V_{l\,nf}$ = approximately 13,400 m^3

The intermediate volume values correspond to an uncertainty domain where the statistical analysis of the literature includes both cases of formation and non-formation of river barriers (Figure 6).

3.2.2. *HDSI* Index Analysis

Subsequently, the *HDSI* index was used to calculate the threshold volumes characterizing the stability or instability of a possible river dam. Using ArcGIS Pro$^{®}$ software, the DTM was processed to derive the flow accumulation raster for the whole area. As a result, it was possible to identify the area of the basin upstream of the previously identified critical section (Figure 7) as:

$$A_b = 234.3 \text{ km}^2$$
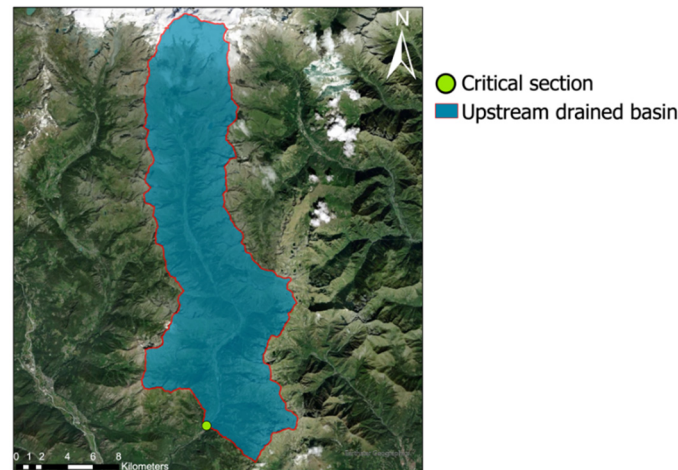
Figure 7. Drained watershed upstream of the critical section identified at the footslope of Theilly landslide.

The other morphometric parameter needed to assess the *HDSI* index is the local slope gradient of the riverbed at the critical section (*S*). It was derived from the DTM using the corresponding function of ArcGIS Pro, resulting in the value $S = 5.1°$.

To estimate the threshold volumes for the dam stability and instability, the threshold values of the *HDSI* parameter identified by [26] were considered: *HDSI* = 7.44 defines the stability domain and *HDSI* = 5.74 the instability domain. The *HDSI* formula (Equation (3)) was solved for the volume:

$$V = tan(S) * A_b * 10^{HDSI} \tag{7}$$

After substituting the threshold *HDSI* values and the values of the hydro-morphometric indices (*S* and A_b) characterizing the test site, the following results were obtained:

- Stability critical volume (for *HDSI* = 7.44): $V_{lst} = 5.76 * 10^8$ m^3
- Instability critical volume (for *HDSI* = 5.74): $V_{linst} = 1.15 * 10^7$ m^3

Volumes greater than V_{lst} can be correlated with a stable dam in the long term, values lower than V_{linst} can be associated with an unstable dam, for intermediate values the evolution is uncertain.

From a graphical point of view, the results can be displayed in a graph (Figure 8) by setting the product $A_b * tan(S)$ on the x-axis (intrinsic condition of the critical section

threatened by the Thielly landslide) and deriving the corresponding threshold volumes on the y-axis.
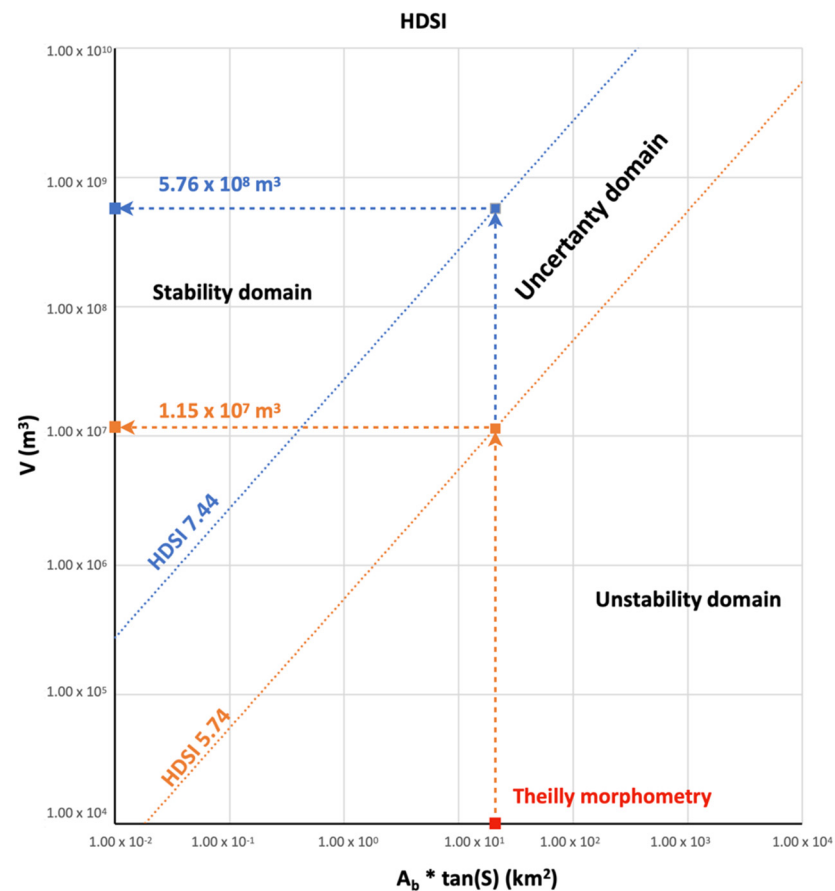
Figure 8. *HDSI* index graph and identification of the threshold volumes for this case of study.

4. Discussion

The outcome of the analyses can be temporarily used for hazard management of Thielly landslides until more complex analyses (including geo-gnostic campaigns) are accomplished.

The proposed set of rainfall thresholds can be used for monitoring purposes by using the automatic real-time rainfall records of the reference rain gauge and, in case a projection for the next days is desired, combining also the rainfall forecasts disseminated at least daily by the Regional Functional Center (the office in charge of weather monitoring, forecasting, and surveillance). These rainfall values can be easily compared with the set of thresholds to derive the expected scenario and the most appropriate form of intervention:

- If the thresholds are not overcome, no relevant event is expected.
- If the lower threshold (ordinary criticality) is overcome, the minimum rainfall conditions for landslide triggering are reached: it is possible that mass movements or erosional processes are reactivated along the slope. However, their occurrence is not certain, and the occurrence of false alarms is also likely, as demonstrated by the empirical calibration procedure. No counteraction is expected except for intensifying the monitoring duty.
- If the moderate criticality threshold is overcome, the reactivation of mass movements or severe erosional processes should be expected. Local authorities should be contacted to receive a first-hand description of the evolution of the hazard scenario.
- When the high criticality threshold is overcome, the reactivation of larger mass movements or severe erosive processes should be expected. In addition to the aforementioned actions, an inspection to the site is recommended during or shortly after the event, and extraordinary maintenance should be performed on the remedial works

and on the surroundings of the slope (e.g., cleaning of the drainages and outlets, removal of debris, and so on).

In the event of a landslide detaching from the slope, it is possible to make a quick estimate of the interaction with the Lys river, based on the volume of the landslide that reaches the riverbed:

- for volumes less than 13,400 m^3, a river dam would not form;
- from 13,400 m^3 to 236,000 m^3, the river dam formation is uncertain, and in the case of formation, the dam would be unstable;
- from 236,000 m^3 to 11.5×10^6 m^3, an unstable river dam would form;
- from 11.5×10^6 m^3 to 576×10^6 m^3, a dam would form with uncertain evolution;
- over 576×10^6 m^3, a dam would form and would be stable even in the long term.

Based on field inspections and on the analysis of the documentation of past landslide events in Theilly (technical reports, event reports, newspapers), it seems unlikely that the dynamics of the slope could evolve into the detachment of a single mass greater than 13,000 m^3 that would entirely reach the Lys riverbed. Therefore, in general terms, the formation of river dams due to the evolution of the slope of this study could be considered unlikely. Moreover, in the event of a mass movement, it is possible to estimate the volumes involved and compare them with the threshold values shown above, in order to have quick feedback on the evolution of the phenomenon.

5. Conclusions

The slope below the village of Theilly, located in the Western Italian Alps, has traditionally been affected by erosion and landslide processes. Recently (since 2016), several reactivations occurred and required the quick development of methods to assess the hazard associated with the site, namely the reactivation of mass movements and the possibility of damming the river at the footslope. Therefore, some recently developed empirical methods were applied and customized for the Theilly case study. An empirical procedure called MaCumBA [42] was applied to derive an intensity–duration rainfall threshold to identify the minimum rainfall conditions associated with slope instabilities. By means of a site-specific empirical calibration, the threshold was further developed into a set of three thresholds, which identify four criticality levels, each connected to an expected event scenario and a corresponding suggested countermeasure from the operational point of view. The interaction between the landslide and the river flowing at the footslope was assessed by means of a set of recently proposed empirical hydro-morphometric indices [26], which were applied to the case of study with an innovative approach, to identify a set of threshold values of the landslide volume for which, if a landslide would reach the riverbed, the following scenarios should be expected: (i) formation of a stable dam, (ii) formation of an unstable dam, (iii) no river barrier formation.

This manuscript demonstrates that, when time is a crucial factor, empirical methodologies can be reliable options to perform a quick hazard analysis and to assist decision makers. To do so, however, a rigorous site-specific calibration is required, and it should be stressed that such tools should be considered a short-term solution, to be used while more thorough analyses are carried out. Indeed, concerning this case of study, further research is in progress to define a 3D model of the hillslope (by means of geophysics and geotechnical survey) and to perform finite element slope stability modeling, with the objective to gain advanced knowledge of the slope characteristics before designing appropriate remedial works. These activities are costly and time consuming; therefore, the proposed methods were based on easily available input data and the outcomes quickly provided a set of tools that could be readily used to forecast the evolution of Theilly landslide and temporarily manage the associated multi-hazards until definitive remedial works are designed and completed.

References

1. Schuster, R.L. Socioeconomic and environmental impacts of landslide. In *Landslides Investigation and Mitigation*, 1st ed.; Turner, A.K., Schuster, R.L., Eds.; Transportation Research Board: Washington, DC, USA; Citeseer: Princeton, NJ, USA, 1996; Volume 247, pp. 12–35.
2. Froude, M.J.; Petley, D.N. Global fatal landslide occurrence from 2004 to 2016. *Nat. Hazards Earth Syst. Sci.* **2018**, *18*, 2161–2181. [CrossRef]
3. Haque, U.; da Silva, P.F.; Devoli, G.; Pilz, J.; Zhao, B.; Khaloua, A.; Wilopo, W.; Andersen, P.; Lu, P.; Lee, J.; et al. The human cost of global warming: Deadly landslides and their triggers (1995–2014). *Sci. Total Environ.* **2019**, *682*, 673–684. [CrossRef] [PubMed]
4. Fan, X.; Dufresne, A.; Subramanian, S.S.; Strom, A.; Hermanns, R.; Stefanelli, C.T.; Hewitt, K.; Yunus, A.P.; Dunning, S.; Capra, L.; et al. The formation and impact of landslide dams—State of the art. *Earth-Sci. Rev.* **2020**, *203*, 103116. [CrossRef]
5. Korup, O. Recent research on landslide dams—A literature review with special attention to New Zealand. *Prog. Phys. Geogr. Earth Environ.* **2002**, *26*, 206–235. [CrossRef]
6. Fan, X.; Scaringi, G.; Korup, O.; West, A.J.; Van Westen, C.J.; Tanyas, H.; Hovius, N.; Hales, T.C.; Jibson, R.W.; Allstadt, K.E.; et al. Earthquake-Induced Chains of Geologic Hazards: Patterns, Mechanisms, and Impacts. *Rev. Geophys.* **2019**, *57*, 421–503. [CrossRef]
7. Dai, F.; Lee, C.; Deng, J.; Tham, L. The 1786 earthquake-triggered landslide dam and subsequent dam-break flood on the Dadu River, southwestern China. *Geomorphology* **2005**, *65*, 205–221. [CrossRef]
8. Chae, B.-G.; Park, H.-J.; Catani, F.; Simoni, A.; Berti, M. Landslide prediction, monitoring and early warning: A concise review of state-of-the-art. *Geosci. J.* **2017**, *21*, 1033–1070. [CrossRef]
9. Segoni, S.; Piciullo, L.; Gariano, S.L. A review of the recent literature on rainfall thresholds for landslide occurrence. *Landslides* **2018**, *15*, 1483–1501. [CrossRef]
10. Aleotti, P.; Chowdhury, R. Landslide hazard assessment: Summary review and new perspectives. *Bull. Eng. Geol. Environ.* **1999**, *58*, 21–44. [CrossRef]
11. Catani, F.; Segoni, S. Prediction and Forecasting of Mass-Movements. In *Treatise on Geomorphology*; Elsevier: Amsterdam, The Netherlands, 2022; pp. 531–545. [CrossRef]
12. Piciullo, L.; Calvello, M.; Cepeda, J.M. Territorial early warning systems for rainfall-induced landslides. *Earth Sci. Rev.* **2018**, *179*, 228–247. [CrossRef]
13. Guzzetti, F.; Gariano, S.L.; Peruccacci, S.; Brunetti, M.T.; Marchesini, I.; Rossi, M.; Melillo, M. Geographical landslide early warning systems. *Earth-Sci. Rev.* **2020**, *200*, 102973. [CrossRef]
14. Caine, N. The Rainfall Intensity—Duration Control of Shallow Landslides and Debris Flows. *Geogr. Ann. Ser. A Phys. Geogr.* **1980**, *62*, 23–27. [CrossRef]
15. Tiranti, D.; Rabuffetti, D. Estimation of rainfall thresholds triggering shallow landslides for an operational warning system implementation. *Landslides* **2010**, *7*, 471–481. [CrossRef]
16. Devoli, G.; Tiranti, D.; Cremonini, R.; Sund, M.; Boje, S. Comparison of landslide forecasting services in Piedmont (Italy) and Norway, illustrated by events in late spring 2013. *Nat. Hazards Earth Syst. Sci.* **2018**, *18*, 1351–1372. [CrossRef]
17. Kong, V.W.W.; Kwan, J.S.H.; Pun, W.K. Hong Kong's landslip warning system—40 years of progress. *Landslides* **2020**, *17*, 1453–1463. [CrossRef]
18. Gariano, S.L.; Brunetti, M.T.; Iovine, G.; Melillo, M.; Peruccacci, S.; Terranova, O.; Vennari, C.; Guzzetti, F. Calibration and validation of rainfall thresholds for shallow landslide forecasting in Sicily, southern Italy. *Geomorphology* **2015**, *228*, 653–665. [CrossRef]
19. Fan, X.; Dufresne, A.; Whiteley, J.; Yunus, A.P.; Subramanian, S.S.; Okeke, C.A.; Pánek, T.; Hermanns, R.L.; Ming, P.; Strom, A.; et al. Recent technological and methodological advances for the investigation of landslide dams. *Earth-Sci. Rev.* **2021**, *218*, 103646. [CrossRef]

20. Zheng, H.; Shi, Z.; Shen, D.; Peng, M.; Hanley, K.J.; Ma, C.; Zhang, L. Recent Advances in Stability and Failure Mechanisms of Landslide Dams. *Front. Earth Sci.* **2021**, *9*, 659935. [CrossRef]

21. Braun, A.; Cuomo, S.; Petrosino, S.; Wang, X.; Zhang, L. Numerical SPH analysis of debris flow run-out and related river damming scenarios for a local case study in SW China. *Landslides* **2018**, *15*, 535–550. [CrossRef]

22. Swanson, F.J.; Oyagi, N.; Tominaga, M. Landslide dams in Japan. In *Landslide Dams: Processes, Risk, and Mitigation*; ASCE: Reston, VA, USA, 1986; pp. 131–145.

23. Ermini, L.; Casagli, N. Prediction of the behaviour of landslide dams using a geomorphological dimensionless index. *Earth Surf. Process. Landf.* **2003**, *28*, 31–47. [CrossRef]

24. Liao, H.-M.; Yang, X.-G.; Xu, F.-G.; Xu, H.; Zhou, J.-W. A fuzzy comprehensive method for the risk assessment of a landslide-dammed lake. *Environ. Earth Sci.* **2018**, *77*, 750. [CrossRef]

25. Korup, O. Geomorphometric characteristics of New Zealand landslide dams. *Eng. Geol.* **2004**, *73*, 13–35. [CrossRef]

26. Stefanelli, C.T.; Segoni, S.; Casagli, N.; Catani, F. Geomorphic indexing of landslide dams evolution. *Eng. Geol.* **2016**, *208*, 1–10. [CrossRef]

27. Corominas, J.; Moya, J. Reconstructing recent landslide activity in relation to rainfall in the Llobregat River basin, Eastern Pyrenees, Spain. *Geomorphology* **1999**, *30*, 79–93. [CrossRef]

28. Giannecchini, R.; Galanti, Y.; D'Amato Avanzi, G. Critical rainfall thresholds for triggering shallow landslides in the Serchio River Valley (Tuscany, Italy). *Nat. Hazards Earth Syst. Sci.* **2012**, *12*, 829–842. [CrossRef]

29. Rosi, A.; Canavesi, V.; Segoni, S.; Nery, T.D.; Catani, F.; Casagli, N. Landslides in the Mountain Region of Rio de Janeiro: A Proposal for the Semi-Automated Definition of Multiple Rainfall Thresholds. *Geosciences* **2019**, *9*, 203. [CrossRef]

30. Lee, S.; Won, J.-S.; Jeon, S.; Park, I.; Lee, M.J. Spatial Landslide Hazard Prediction Using Rainfall Probability and a Logistic Regression Model. *Math. Geol.* **2015**, *47*, 565–589. [CrossRef]

31. Ma, C.; Hu, K.-H.; Zou, Q.; Tian, M. Characteristics of clustering debris flows in Wenchuan earthquake zone. *J. Mt. Sci.* **2013**, *10*, 953–961. [CrossRef]

32. Guzzetti, F.; Peruccacci, S.; Rossi, M.; Stark, C.P. The rainfall intensity–duration control of shallow landslides and debris flows: An update. *Landslides* **2008**, *5*, 3–17. [CrossRef]

33. Zêzere, J.L.; Vaz, T.; Pereira, S.; Oliveira, S.C.; Marques, R.; Garcia, R.A.C. Rainfall thresholds for landslide activity in Portugal: A state of the art. *Environ. Earth Sci.* **2015**, *73*, 2917–2936. [CrossRef]

34. Tiranti, D.; Nicolò, G.; Gaeta, A.R. Shallow landslides predisposing and triggering factors in developing a regional early warning system. *Landslides* **2019**, *16*, 235–251. [CrossRef]

35. Sengupta, A.; Gupta, S.; Anbarasu, K. Rainfall thresholds for the initiation of landslide at Lanta Khola in north Sikkim, India. *Nat. Hazards* **2010**, *52*, 31–42. [CrossRef]

36. Chen, H.; Wang, J. Regression analyses for the minimum intensity-duration conditions of continuous rainfall for mudflows triggering in Yan'an, northern Shaanxi (China). *Bull. Eng. Geol. Environ.* **2014**, *73*, 917–928. [CrossRef]

37. Franceschini, R.; Rosi, A.; Catani, F.; Casagli, N. Exploring a landslide inventory created by automated web data mining: The case of Italy. *Landslides* **2022**, *19*, 841–853. [CrossRef]

38. Battistini, A.; Rosi, A.; Segoni, S.; Lagomarsino, D.; Catani, F.; Casagli, N. Validation of landslide hazard models using a semantic engine on online news. *Appl. Geogr.* **2017**, *82*, 59–65. [CrossRef]

39. Abraham, M.T.; Satyam, N.; Rosi, A.; Pradhan, B.; Segoni, S. The Selection of Rain Gauges and Rainfall Parameters in Estimating Intensity-Duration Thresholds for Landslide Occurrence: Case Study from Wayanad (India). *Water* **2020**, *12*, 1000. [CrossRef]

40. Gariano, S.L.; Melillo, M.; Peruccacci, S.; Brunetti, M.T. How much does the rainfall temporal resolution affect rainfall thresholds for landslide triggering? *Nat. Hazards* **2020**, *100*, 655–670. [CrossRef]

41. Rossi, M.; Luciani, S.; Valigi, D.; Kirschbaum, D.; Brunetti, M.; Peruccacci, S.; Guzzetti, F. Statistical approaches for the definition of landslide rainfall thresholds and their uncertainty using rain gauge and satellite data. *Geomorphology* **2017**, *285*, 16–27. [CrossRef]

42. Segoni, S.; Rossi, G.; Rosi, A.; Catani, F. Landslides triggered by rainfall: A semi-automated procedure to define consistent intensity–duration thresholds. *Comput. Geosci.* **2014**, *63*, 123–131. [CrossRef]